Progress in Medical Devices
eISSN:2957-5478

Review Article https://doi.org/10.61189/036308mdyran

Research progress on medical ultrasound image segmentation algorithms

Tianfeng Dong[1], Shiju Yan[1], Hengyu Li[2], Sheng Yuan[1]

[1]School of Health Science and Engineering, University of Shanghai for Science and Technology, Shanghai 200093, China. [2]Department of Breast and Thyroid Surgery, Changhai Hospital, Second Military Medical University/Naval Medical University, Shanghai 200433, China.

Corresponding author: Shiju Yan.

Declaration of conflict of interest: None.

Received May 8, 2023; Accepted November 23, 2023; Published December 31, 2023

Highlights

- Medical image segmentation algorithms play a crucial role in diagnosing and screening lesions.
- Appropriate segmentation techniques are conducive to reducing the workload of doctors and hold significant im plications for clinical auxiliary treatment.

Abstract

Medical ultrasound imaging is an integral part of preoperative diagnosis, lesion screening and ultrasound-guided interventional surgeries. Image segmentation techniques can enhance the identification of lesions and separate them from complex backgrounds, aiding physicians in both quantitative and qualitative analyses. Ultrasound image segmentation algorithms are primarily categorized into two types: traditional non-semantic segmentation and deep learning-based semantic segmentation, each with distinct advantages and drawbacks. This paper delves into these segmentation principles, elucidating their relevance in the realm of ultrasound image segmentation, and offers an overview of current research trends. Our goal is to provide guidance for physicians and researchers in selecting the most suitable segmentation algorithm that tailors to their specific requirements.

Keywords: Ultrasound imaging, deep learning, semantic segmentation, developmental trends

Introduction

Ultrasound has emerged as a pivotal modality in contemporary medicine due to its efficacy in imaging soft and muscular tissues. It has the advantages of rapid imaging, cost-effectiveness, absence of radiation, and real-time visualization of soft tissue structures compared to X-ray. Previously, mammography was the most effective tool for early detection of breast cancer, but it has obvious limitations, leading to misdiagnosis and many unnecessary biopsies (65-85%), as well as missed diagnoses, where 10-30% breast cancers were not detected in time [1-3]. Therefore, ultrasound imaging has become an important alternative to mammography. Research has shown that over one fourth of studies utilized ultrasound images, with the ratio growing at an accelerated rate [4]. Evidence suggests that ultrasound images are effective in differentiating benign from malignant tumors with high accuracy [5]. Additionally, they enhance the cancer detection rate by 17% and reduce unnecessary biopsies by 40% [6, 7].

However, ultrasound image interpretation requires well-trained and experienced radiologists. Even well-trained experts may have a high inter-observer variation rate. In recent years, computer-aided diagnosis has made great strides driven by advancements in computer technology, encompassing both computer vision and artificial intelligence [8]. Through computer-aided diagnosis, it is feasible to differentiate between benign and malignant breast tumors by analyzing their boundaries and morphology [9]. Moreover, segmentation

Address correspondence to: Shiju Yan, School of Health Science and Engineering, University of Shanghai for Science and Technology, No.516, Jungong Road, Yangpu District, Shanghai 200093, China. Tel: 18217617984; E-mail: yanshiju@usst.edu.cn.

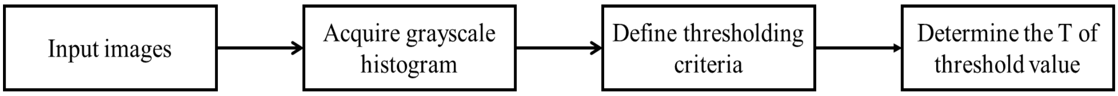

Figure 1. Basic flowchart of threshold segmentation.

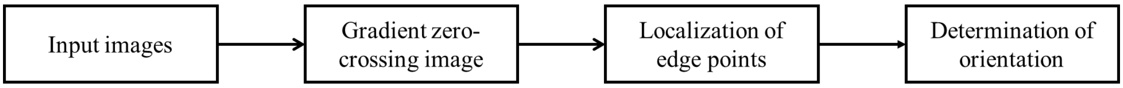

Figure 2. Basic flowchart of edge segmentation using differential operator.

algorithms play a crucial role in identifying needle tips in ultrasound images, potentially reducing and compensating for surgeon fatigue during minimally invasive procedures [10].

Despite the advantages, ultrasound imaging also comes with challenges, namely limited resolution, ambiguous lesion boundaries, and the presence of speckle noise, all of which complicate accurate lesion segmentation. Therefore, accurate segmentation of lesions within ultrasound images remains a pressing challenge. While numerous image segmentation algorithms exist, this paper delves into the diverse domains of current ultrasound image segmentation algorithms and their applications. Furthermore, a summary and future outlook are provided, aiming to serve as a reference for researchers and medical practitioners.

Methods

Non-Semantic Ultrasound Image Segmentation

Traditional image segmentation algorithms rely on fundamental features, such as color and texture, to segment desired objects or regions. Owing to their high computational efficiency and consistent performance, these techniques have emerged as predominant in image segmentation applications. Notably, techniques rooted in edge detection, regional attributes and deformation models are commonly employed.

Edge-Based Ultrasound Image Segmentation

Edge-based image segmentation algorithms identify edges by analyzing the distinctiveness of pixels across different regions, primarily using threshold segmentation and differential operators.

Threshold segmentation stands out due to its ubiquitous applicability and foundational principle: discernible grey-scale disparities exist between foreground and background regions, which allows for the determination of a suitable threshold, T, differentiating the foreground from the background, as shown in **Figure 1** [11]. The Otsu method optimizes segmentation by selecting a threshold, T, that maximizes or minimizes the interclass variance across distinct regions [12]. An enhancement to the Otsu algorithm, as detailed by Hui-Fuang Ng, ensures that the threshold, T, aligns optimally with the valley of variance [13]. In ultrasound image, lesions exhibit a notably denser grey value distribution. The maximum entropy thresholding algorithm exploits this density, calculating the information entropy of image to pinpoint the ideal threshold, T, at the position of maximum entropy [14].

Local differential operators, including the Laplacian, Sobel, and Canny operators, facilitate edge detection for image segmentation [15, 16]. As shown in **Figure 2**, these operators operate on the premise that first-order derivatives present extreme values at greyscale transitions, while second-order derivatives manifest non-zero points. However, in ultrasound image, the inherent discontinuity and high-frequency noise complicate lesion edge identification when relying solely on differential operators. To address these challenges, several enhancements have been proposed. For instance, researchers have utilized the nonlinear Laplacian operator to identify pixels associated with second-order derivative changes and augmented edge pixel definition for better segmentation [17]. Additionally, Fan et al. introduced nonlinear wavelets for segmenting the inner and outer boundaries of tubular artery ultrasound images [18].

Region-Based Ultrasound Image Segmentation

As shown in **Figure 3**, region-based algorithms offer a method for image segmentation, encompassing both the region growth and watershed algorithms. These algorithms segment images based on internal region similarity. Specifically, the region-growing algorithm identifies seed pixels through a defined growth criterion. It then amalgamates pixels sharing similar characteristics across disparate regions, forming

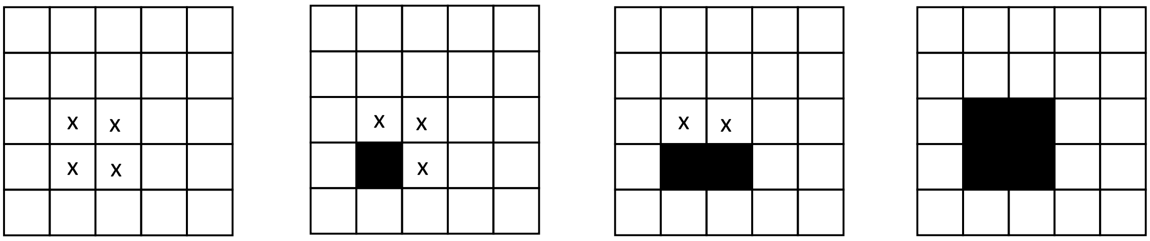

Figure 3. Region growing algorithm.

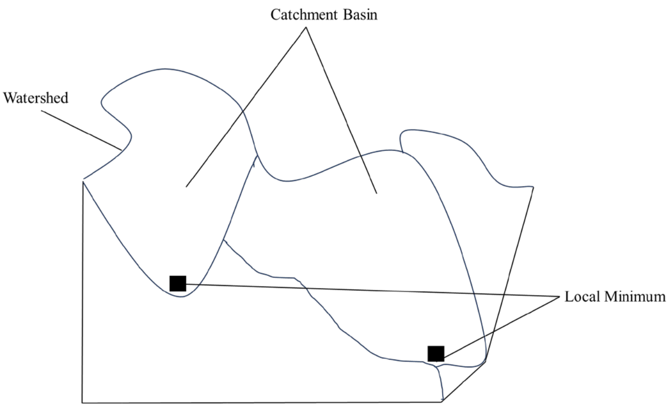

Figure 4. Watershed algorithm.

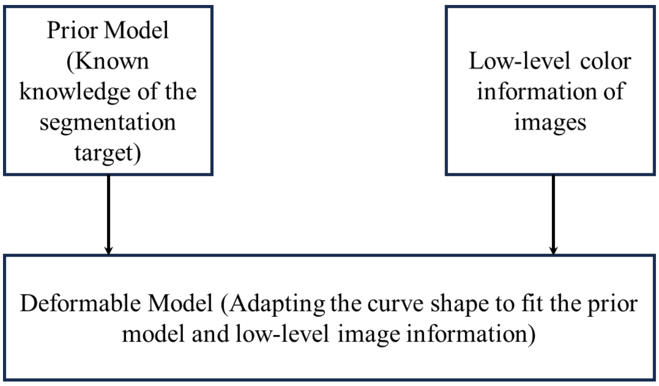

Figure 5. Basic flowchart of deformation model segmentation.

distinct regions for ultrasound image segmentation [19]. Fan et al. introduced a method that incorporates two constraints to autonomously identify seed pixels within breast tumor lesions [20]. This method innovatively merges iterative quadrinomial tree decomposition with greyscale values, thereby enhancing the segmentation of ultrasound image lesions.

As shown in **Figure 4**, the watershed algorithm, commonly referred to as watershed segmentation, interprets the grayscale of an image as analogous to the topographical features of the surface of earth, with the grayscale values representing a third-dimensional elevation perspective [21]. Though prevalently employed in pattern recognition and medical imaging, the watershed method frequently suffers from over-segmentation. To counteract this, Weickert et al. introduced a region-merging approach as an enhancement [22]. Additionally, the challenge of over-segmentation was tackled by Jung et al. through an integration of the watershed algorithm with wavelet transform [23]. Further, Gomez et al. applied the watershed algorithm to segment breast ultrasound images by using constraints on the textural features derived from the Gabor filter [24].

Deformation Model-Based Ultrasound Image Segmentation

The concept of deformation model draws inspiration from physics and geometric theories. This model assimilates relevant grayscale and texture information from image data to segment targets following predefined criteria, as shown in **Figure 5**.

The active contour model, often referred to as the snake model, provides a robust framework for delineating the contour of an image target through the minimization or maximization of an energy functional [25]. The curve evolution process of this model autonomously determinate the interior of the curve and maintains its smooth transition. An external force guides the curve towards the boundaries of the region of interest (ROI), as influenced by the image's constraints and potential energy.

The region-based active contour Chan-Vese model was proposed by Wang et al. [26]. The Chan-Vese model proposed by Hmida et al. incorporates a new segmentation algorithm to obtain a model that depicts the contour of the mass [27]. Specifically, Kuo et al. segmented breast ultrasound images using radial gradient index contour [28]. Gu et al. proposed an improved approach based on the aforementioned algorithm by providing an edge-based deformation model [29]. To accurately track the local changes in grayscale

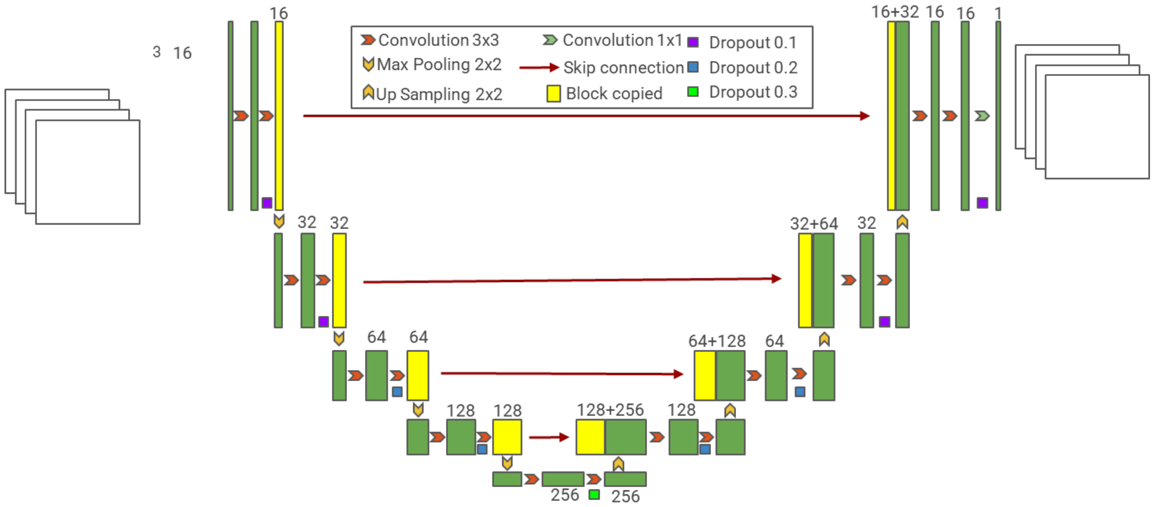

Figure 6. U-Net model.

in the ultrasound image, Li et al. utilized the local attribute of the kernel function, based on the region-scalable fitting method [30]. This algorithm is highly effective in segmenting images with uneven grayscale distributions. Moreover, an active contour model based on Bhattacharyya gradient flow was proposed to treat the target area and background area of images as different samples [31]. To achieve the goal of image segmentation without depending on the uniformity information of the super-grayscale image, the issue is transformed into a probabilistic model problem by computing the Babbitt distance between the two sample distributions. Yuan et al. proposed a model called region-scalable fitting and Bhattacharyya distance that combines the benefits of the region-scalable fitting model and the Bhattacharyya gradient flow model to solve the problem of uneven gray levels and blurring borders in ultrasound images [32].

Deep Learning-Based Ultrasound Image Segmentation

Convolutional neural networks (CNNs) are a specialized category in deep learning architectures designed to process structured grid data, such as images [33]. A typical CNN comprises convolutional layers, pooling layers, and fully connected layers. This design equips CNNs with robust feature extraction and data abstraction capabilities. Instead of relying on handcrafted features, CNNs can automatically recognize correlations between inputs and outputs through adaptive learning, making them particularly suitable for tasks such as image segmentation and classification.

U-Shaped and Its Derivative Networks

U-Net represents a pivotal advancement in medical image segmentation and continues to be a prominent semantic segmentation algorithm, as shown in **Figure 6** [34]. Within its architecture, the shallow convolutional layers predominantly capture spatial and textural nuances due to their limited receptive field and high-resolution capacity. In contrast, the deep convolutional layers can discern broader semantic features, facilitated by an expansive receptive field and lower resolution. Distinctively, U-Net exhibits a symmetrical encoder-decoder configuration, fostering an integration between shallow and deep feature representations. This architectural nuance equips U-Net with the capability to concurrently process both texture-oriented features and high-level semantic features, thereby augmenting its receptive field and enhancing segmentation precision.

Various enhancements have been proposed to bolster the original U-Net architecture. The recurrent residual U-Net addresses the degradation in segmentation results that attributed to gradient explosion or vanishing, particularly as the network deepens [35]. Furthermore, the adoption of Prelu as an activation function has been suggested to optimize the network's performance. Karthik et al. introduced a multi-level U-Net, which is capable of real-time segmentation of breast masses in ultrasound images [36]. U-Net++ innovatively incorporates a dense connection between each convolutional layer, performing upsampling and feature fusion on the encoder-generated feature map to bridge the disparity between the encoder and the decoder [37, 38]. In a different approach, residual U-Net employs the residual network as its backbone, enhancing the convolution module traditionally used in U-Net [39, 40]. Building

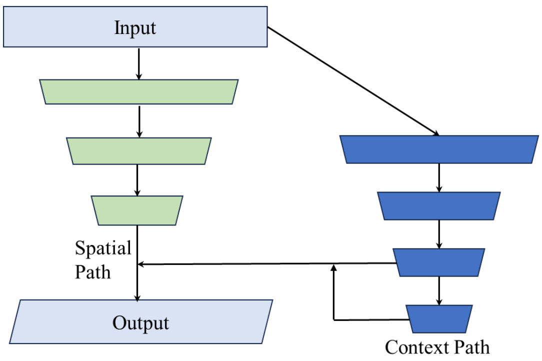

Figure 7. The spatial path and context path of BiSeNet .

upon this, ResUNet++ integrates a squeeze and extraction block to emphasize pivotal channels within the network, consequently suppressing less significant ones [41, 42]. Furthermore, the SK-U-Net approach refines the ROI of network towards the lesion using channel attention, resulting in the selective kernel module delivering superior segmentation outcomes during the segmentation of lesions in ultrasound breast images [43].

Advancements in U-Net data processing techniques are well documented, with a specific emphasis on data augmentation strategies. Zeiser et al. detailed an approach that enhances data through techniques such as contrast enhancement and flipping, while concurrently removing extraneous information from images by using U-Net [44]. In the more recent development, nnU-Net accentuates the significance of data augmentation [45]. Rather than primarily focusing on the model, nnU-Net is dedicated to understand how varying segmentation tasks influence the final resulting segmentation. Consequently, nnUnet prioritizes data pre-processing, post-processing, and tailoring hyperparameter settings to cater to specific models for different tasks. This comprehensive approach aims to elevate both the efficiency and accuracy of segmentation tasks. Presently, the segmentation outcomes from nnUnet have become a benchmark for evaluating novel segmentation models.

Lightweight Networks

Fully convolutional network (FCN) represents a paradigm shift in image segmentation, notably decreasing computational demands by substituting the fully connected layers found in traditional CNNs with convolutional layers [46]. In SegNet, the deconvolution inherent to FCN is superseded by upsampling through nonlinear interpolation, further mitigating computational demands [47]. However, the existing parameter-intensive nature of these models constrains their applicability for real-time processing in scenarios like clinical surgeries or mobile ultrasound-embedded devices.

In this context, Hu et al. reported an efficacious application of BiSeNet for segmenting pediatric ultrasound images of the left and right ventricles, demonstrating superior speed and accuracy relative to U-Net [48, 49]. BiSeNet introduces a bidirectional segmentation framework that coordinates two pathways: the spatial path and the context path as shown in **Figure 7**. The spatial path emphasizes the preservation of spatially rich feature maps, while the context path rapidly downsamples to assimilate high-level semantic information, culminating in an expansive perceptual field via global average pooling.

BiSeNet V2 refines this framework through incorporating a guided aggregation layer to bolster the synergy of spatial and semantic features [50]. Additionally, it enriches both spatial and semantic branches, interweaving an attention mechanism to amplify speed and precision. An insightful deviation is presented in “Rethinking BiseNet” where the short-term dense concatenate module is posited as the backbone network, replacing the classification-centric backbone of BiSeNet [51]. This architectural shift, enabled by the short-term dense concatenate module, markedly amplifies network performance, granting an expansive receptive field with a constrained parameter set.

Applications in Ultrasound Image Segmentation

Image Segmentation in Coronary Artery Disease

Vascular ultrasound is instrumental in the management of coronary artery disease. Its utility extends from the detailed delineation of coronary artery anatomy, providing critical guidance in the selection and evaluation of interventional strategies. The imaging modality offers an intricate view of blood vessel and tissue morphology, allowing clear visualization of structures beneath the intima and accurate measurements of vascular lumen diameters. Given its diagnostic accuracy, segmentation of vascular tissue structures is of paramount importance.

Sonka et al. employed the snake algorithm for coronary artery segmentation, incorporating prior knowledge of vessel cross-sections during model deformation [52]. This knowledge encompasses target edges, shapes, edge orientations, and vessel wall thickness, reflecting manual segmentation procedures. In the study of Bouma et al., a lumen segmentation algorithm was proposed, combining a suite of filtering techniques: Gaussian, median, and anisotropic filters [53]. Coupled with distinct segmentation methodologies, including the threshold, region expansion, and discrete active contour methods, the algorithm's performance was evaluated by experts [54]. However, its efficacy is compromised in the presence of significant image noise, resulting in suboptimal segmentation outcomes relative to expert-driven benchmarks. Pardo et al. introduced a statistical deformation model tailored for coronary artery segmentation by using a derived Gaussian filter for local edge delineation in varying directions [55]. This approach contrasts image features with established knowledge, guiding the deformation using linear discriminant analysis. This optimization streamlines the feature space and enhances the robustness of the model.

Yang et al. introduced an innovative approach dubbed "intravascular ultrasound segmentation network" for coronary artery segmentation using deep learning [56]. The network is rooted in the FCN architecture and employs an aggregated multi-branch structure, integrating features from both U-Net and SegNet in a symmetric layout. The encoding segment comprises four distinct modules, while the decoding segment consists of three. Crucially, skip connections are employed to furnish the decoder with supplementary information. Post-segmentation, an elliptical contour fitting process further refines the result. Compared to conventional methods, intravascular ultrasound segmentation network notably enhances segmentation accuracy.

Breast Ultrasound Image Segmentation

The abundant adipose tissue in breast causes over-segmentation, unclear lesion borders, low contrast, and increased shadows. As a solution to these issues, a three-step method for breast mass segmentation based on superpixel creation and curve development was proposed [57]. This method is based on the creation of superpixels and curve development, utilizing the simple linear iterative clustering method and density-based spatial clustering of applications with noise for breast mass detection and generating mammogram superpixels. Subsequently, ROI in breast masses are constructed, followed by a fitting approach based on local Gaussian distribution to capture the edge of the breast tumor through graphic block processing and spatial constraints. This method effectively eliminates the false positive region of the ROI and provides improved segmentation results by capturing the margin of the breast tumor more accurately.

Wang et al. proposed a novel solution to the complex issue of detecting malignancies in breast ultrasound images: the multi-level nested pyramid network (MNPNet) [58]. The center of MNPNet's design is an encoder module that integrates both ResNet34 and atrous spatial pyramid pooling modules. This configuration ensures efficient encoding of context features from multiple levels, capturing both low-level details and high-level semantic information. On the other hand, the decoder module uses bilinear upsampling and a feature fusion technique, enhancing the segmentation precision of tumor border regions. Collectively, the MNPNet framework outperforms other methods in breast imaging analysis and holds promise for improving diagnostic accuracy in clinical practice.

Ultrasound-Guided Interventional Surgery

Ultrasound-guided minimally invasive surgery employs specialized puncture needles to access lesions through the skin, facilitating procedures like radiofrequency thermal ablation and needle puncture biopsy [59, 60]. This technique allows for localized treatment and minimally invasive surgical intervention on tumor lesions. Notable benefits include the absence of radiation exposure, rapid recovery, and cost-effectiveness. However, inherent challenges of original ultrasound images, such as low resolution, high noise, and difficulty pinpointing lesion locations, still exist. Consequently, during surgery, physicians must continuously monitor the position of the tip of the puncture needle, which is critical to the success of the operation. Thus, compared to other surgical procedures, ultrasound-guided minimally invasive surgery tends to be more reliant on the surgeon's experience.

To accurately pinpoint the position of the puncture needle in real-time during surgery, Mwikirize et al. broke the process down into three stages [61]. First, the movement of the needle tip was identified and amplified within the ultrasound image, keeping the needle tip component in the foreground and relegating the rest to the background. Second, a regularization

Table 1. Summary of traditional non-semantic segmentation algorithms

Algorithm reference	Algorithm type	Algorithm overview
Ng HF. 2006 [13]	Threshold segmentation algorithm	Identifying an appropriate threshold value, T, where inter-class variance between regions is maximized or minimized.
Kapur et al. 1988 [15]	Threshold segmentation algorithm	Utilizing the maximum entropy threshold segmentation algorithm.
Aarnink et al. 1994 [17]	Edge detection segmentation algorithm	Segmenting edge pixels using the nonlinear Laplacian operator for second-order derivative boundaries.
Fan et al. 1996 [18]	Edge detection segmentation algorithm	Segmenting edge pixels using nonlinear wavelet detection.
Fan et al. 2019 [20]	Region segmentation algorithm	Using iterative quadrinomial tree decomposition with grayscale features to establish two constraint conditions for automatic seed pixel identification.
Gomez et al. 2010 [24]	Region segmentation algorithm	Using texture features generated by Gaussian-constrained Gabor filters combined with the Watershed algorithm for segmentation.
Kuo et al. 2013 [28]	Deformable model	Contour segmentation using the Radial Gradient Index.
Yuan J. 2012 [32]	Deformable model	Introducing the region-scalable fitting and Bhattacharyya distance model, merging region-scalable fitting and Bhattacharyya gradient flow benefits, to tackle uneven grayscale and blurriness

Table 2. Summary of deep learning semantic segmentation algorithms

Algorithm reference	Algorithm type	Algorithm overview
Ronneberger O et al. 2015 [34]	U-Net model	Using symmetrical U-shape with skip connections to merge shallow and deep features
Zhou Z et al. 2018 [37]	U-Net model	Added dense connections between convolutional layers.
Zhang Z et al. 2018 [39]	U-Net model	Replacing Backbone with Residual Network
Isensee F et al. 2021 [45]	U-Net model	Emphasizing data pre/post-processing and task-specific hyperparameter tuning
Badrinarayanan V et al. 2017 [47]	Lightweight network	Upsample with nonlinear interpolation, reducing computations.
Yu C et al. 2018 [49]	Lightweight network	Bidirectional segmentation for space info retention and wider receptive field.
Yu C et al. 2021 [50]	Lightweight network	Enhanced spatial and semantic branches with attention mechanism.

filter was deployed to further emphasize the tip and extracted its form features. Finally, the modified Yolo network architecture was utilized to localize the needle tip within the original ultrasound image [62]. On the other hand, Mwikirize recommended classifying the needle tip before any augmentation [63]. If there's spatial movement, the tip is enhanced; otherwise, it remains untouched. This selective approach avoids enhancing every frame, thereby reducing computational demands and accelerating the process.

Summary and outlook

Summary

This paper provides an overview of several ultrasound image segmentation algorithms employed in the realm of medical ultrasound, highlighting their evolution alongside advances in computer technology. Each algorithm presents its own strengths and weaknesses.

The traditional non-semantic image segmentation algorithm is both straightforward and swift. The main traditional non-semantic segmentation algorithms are shown in **Table 1**. They perform effectively on individual images where there's a pronounced contrast between the lesion and the surrounding regions. However, these traditional methods struggle to process ultrasound images with complex composition and high noise, posing challenges like unclear border segmentation.

The deformation model improves the accuracy of ultrasound image segmentation. Nevertheless, it comes with its own drawbacks, such as intricate computations, inability to achieve automatic segmentation, and imprecise boundary tracking.

Deep learning-based segmentation stands out for its superior quality and speed. The main deep learning semantic segmentation algorithms are shown in **Table 2**. By using a lightweight network, it can achieve fully automated segmentation in real-time. The main challenge here lies in the initial phase: a substantial amount of manually labeled data are essential for training the neural network.

Outlook

Effective ultrasound image segmentation aims to improve automated segmentation performance, enhance segmentation accuracy, and reduce computational demands. While critical to the creation and analysis of medical images, this process faces multiple challenges. Conventional algorithms and deformation models often fall short in delivering high-precision segmentation for ultrasound images. Furthermore, the extensive application of deep learning is hindered by the limited availability of medical image data. Additionally, it is also challenging to ideally balance the speed and accuracy for real-time segmentation, limiting its clinical application.

Looking ahead, it's imperative to meld medical knowledge with image segmentation algorithms. Integrating traditional segmentation techniques with deep learning algorithms can be the linchpin for elevating clinical diagnosis efficacy. To counteract the data scarcity issue, datasets can be expanded using unsupervised learning. Future network designs must harmoniously balance speed and accuracy, broadening their applicability in the ultrasound imaging domain.

References

[1] Cheng HD, Shi X, Min R, et al. Approaches for automated detection and classification of masses in mammograms. Pattern Recognit 2006;39:646-668.

[2] Jesneck JL, Lo JY, Baker JA. Breast mass lesions: computer-aided diagnosis models with mammographic and sonographic descriptors. Radiology 2007;244:390-398.

[3] Giger ML. Computer-aided diagnosis in radiology. Acad Radiol 2002;9:1-3.

[4] Chang RF, Wu WJ, Moon WK, et al. Improvement in breast tumor discrimination by support vector machines and speckle-emphasis texture analysis. Ultrasound Med Biol 2003;29:679-686.

[5] Sahiner B, Chan H-P, Roubidoux MA, et al. Malignant and benign breast masses on 3D US volumetric images: effect of computer-aided diagnosis on radiologist accuracy. Radiology 2007;242:716-724.

[6] Drukker K, Giger ML, Horsch K, et al. Computerized lesion detection on breast ultrasound. Med Phys 2002;29:1438-1446.

[7] André MP, Galperin M, Olson LK, et al. Improving the accuracy of diagnostic breast ultrasound. Acoust Imaging 2002;453-460.

[8] Chen HL, Zhou JQ, Chen Q, et al. Comparison of the sensitivity of mammography, ultrasound, magnetic resonance imaging and combinations of these imaging modalities for the detection of small (≤ 2 cm) breast cancer. Medicine 2021;100.

[9] Stoeblen F, Landt S, Ishaq R, et al. High-frequency breast ultrasound for the detection of microcalcifications and associated masses in BI-RADS 4a patients. Anticancer Res 2011;31:2575-2581.

[10] Mwikirize C, Kimbowa AB, Imanirakiza S, et al. Time-aware deep neural networks for needle tip localization in 2D ultrasound. Int J Comput Assist Radiol Surg 2021;16:819-827.

[11] Cheng H-D, Jiang XH, Sun Y, et al. Color image segmentation: advances and prospects. Pattern Recognit 2001;34:2259-2281.

[12] Otsu N. A threshold selection method from gray-level histograms. IEEE Trans Syst Man Cybern 1979;9:62-66.

[13] Ng HF. Automatic thresholding for defect detection. Pattern Recognit Lett 2006;27:1644-1649.

[14] Kapur JN, Sahoo PK, Wong AK. A new method for gray-level picture thresholding using the entropy of the histogram. Comput Vis Graphics Image Process 1985;29:273-285.

[15] Kanopoulos N, Vasanthavada N, Baker RL. Design of an image edge detection filter using the Sobel operator. IEEE J Solid-State Circuits 1988;23:358-367.

[16] Ding L, Goshtasby A. On the Canny edge detector. Pattern Recognit 2001;34:721-725.

[17] Aarnink R, Giesen R, Huynen A, et al. A practical clinical method for contour determination in ultrasonographic prostate images. Ultrasound Med Biol 1994;20:705-717.

[18] Fan L, Braden GA, Herrington DM. Nonlinear wavelet filter for intracoronary ultrasound images. Comput Cardiol 1996 1996;41-44.

[19] Lázár I, Hajdu A. Segmentation of retinal

vessels by means of directional response vector similarity and region growing. Comput Biol Med 2015;66:209-221.
[20] Fan H, Meng F, Liu Y, et al. A novel breast ultrasound image automated segmentation algorithm based on seeded region growing integrating gradual equipartition threshold. Multimedia Tools Appl 2019;78:27915-27932.
[21] Ng H, Ong S, Foong K, et al. Medical image segmentation using k-means clustering and improved watershed algorithm. 2006 IEEE Southwest Symposium on ImageAnalysis and Interpretation 2006;61-65.
[22] Weickert J. Efficient image segmentation using partial differential equations and morphology. Pattern Recognit 2001;34:1813-1824.
[23] Jung CR. Combining wavelets and watersheds for robust multiscale image segmentation. Image Vis Comput 2007;25:24-33.
[24] Gomez W, Leija L, Alvarenga A, et al. Computerized lesion segmentation of breast ultrasound based on marker-controlled watershed transformation. Med Phys 2010;37:82-95.
[25] Kass M, Witkin A, Terzopoulos D. Snakes: Active contour models. Int J Comput Vis 1988;1:321-331.
[26] Wang X-F, Huang D-S, Xu H. An efficient local Chan–Vese model for image segmentation. Pattern Recognit 2010;43:603-618.
[27] Hmida M, Hamrouni K, Solaiman B, et al. Mammographic mass segmentation using fuzzy contours. Comput Methods Programs Biomed 2018;164:131-142.
[28] Kuo HC, Giger ML, Reiser I, et al. Automatic 3D lesion segmentation on breast ultrasound images. Med Imag 2013;8670:555-560.
[29] Gu P, Lee WM, Roubidoux MA, et al. Automated 3D ultrasound image segmentation to aid breast cancer image interpretation. Ultrasonics 2016;65:51-58.
[30] Li C, Kao C-Y, Gore JC, et al. Minimization of region-scalable fitting energy for image segmentation. IEEE Trans Image Process 2008;17:1940-1949.
[31] Michailovich O, Rathi Y, Tannenbaum A. Image segmentation using active contours driven by the Bhattacharyya gradient flow. IEEE Trans Image Process 2007;16:2787-2801.
[32] Yuan J. Active contour driven by region-scalable fitting and local Bhattacharyya distance energies for ultrasound image segmentation. IET Image Process 2012;6:1075-1083.
[33] Shin HC, Roth HR, Gao M, et al. Deep convolutional neural networks for computer-aided detection: CNN architectures, dataset characteristics and transfer learning. IEEE Trans Image Process 2016;35:1285-1298.
[34] Ronneberger O, Fischer P, Brox T. U-net: Convolutional networks for biomedical image segmentation. Lecture Notes in Computer Science (9351): Medical Image Computing and Computer-Assisted Intervention–MICCAI 2015. Springer, Cham 2015.
[35] Alom MZ, Hasan M, Yakopcic C, et al. Recurrent residual convolutional neural network based on u-net (r2u-net) for medical image segmentation (Preprint). ArXiv 2018.
[36] Karthik L, Kumar G, Keswani T, et al. Protease inhibitors from marine actinobacteria as a potential source for antimalarial compound. PloS one 2014;9:e90972.
[37] Zhou Z, Siddiquee MMR, Tajbakhsh N, et al. UNet++: A Nested U-Net Architecture for Medical Image Segmentation. Deep Learn Med Image Anal Multimodal Learn Clin Decis Support (2018) 2018;11045:3-11.
[38] Huang G, Liu Z, Maaten LV, et al. Densely connected convolutional networks. 2017 IEEE Conference on Computer Vision and Pattern Recognition (CVPR) 2017;2261-2269
[39] Zhang Z, Liu Q, Wang Y. Road extraction by deep residual u-net. IEEE Geosci Remote Sens 2018;15:749-753.
[40] He K, Zhang X, Ren S, et al. Deep residual learning for image recognition. 2016 IEEE Conference on Computer Vision and Pattern Recognition (CVPR) 2016;779-778
[41] Jha D, Smedsrud PH, Riegler MA, et al. Resunet++: An advanced architecture for medical image segmentation. 2019 IEEE international symposium on multimedia (ISM) 2019;225-2255.
[42] Hu J, Shen L, Sun G. Squeeze-and-excitation networks. 2018 IEEE/CVF Conference on Computer Vision and Pattern Recognition 2018;7132-7141.
[43] Byra M, Jarosik P, Szubert A, et al. Breast mass segmentation in ultrasound with selective kernel U-Net convolutional neural network. Biomed Signal Process Control 2020;61:102027.
[44] Zeiser FA, da Costa CA, Zonta T, et al. Segmentation of masses on mammograms using data augmentation and deep learning. J Digit Imaging 2020;33:858-868.
[45] Isensee F, Jaeger PF, Kohl SA, et al. nnU-Net: a self-configuring method for deep learning-based biomedical image segmentation. Nat Methods 2021;18:203-211.
[46] Long J, Shelhamer E, Darrell T. Fully convolutional networks for semantic segmentation. 2015 IEEE Conference on Computer Vision and Pattern Recognition (CVPR) 2015;3431-3440.
[47] Badrinarayanan V, Kendall A, Cipolla R. Segnet: A deep convolutional encoder-decoder

architecture for image segmentation. IEEE Trans Pattern Anal Mach Intell 2017;39:2481-2495.

[48] Hu Y, Guo L, Lei B, et al. Fully automatic pediatric echocardiography segmentation using deep convolutional networks based on BiSeNet. 2019 41st Annual International Conference of the IEEE Engineering in Medicine and Biology Society (EMBC) 2019;6561-6564.

[49] Yu C, Wang J, Peng C, et al. Bisenet: Bilateral segmentation network for real-time semantic segmentation. Lecture Notes in Computer Science (11217): Computer Vision–ECCV 2018. Springer, Cham 2018;334-349.

[50] Yu C, Gao C, Wang J, et al. Bisenet v2: Bilateral network with guided aggregation for real-time semantic segmentation. Int J Comput Vis 2021;129:3051-3068.

[51] Fan M, Lai S, Huang J, et al. Rethinking bisenet for real-time semantic segmentation. 2021 IEEE/CVF Conference on Computer Vision and Pattern Recognition (CVPR). 2021;9711-9720.

[52] Sonka M, Zhang X, Siebes M, et al. Segmentation of intravascular ultrasound images: A knowledge-based approach. IEEE Trans Image Process 1995;14:719-732.

[53] Bouma CJ, Niessen WJ, Zuiderveld KJ, et al. Automated lumen definition from 30 MHz intravascular ultrasound images. Med Image Anal 1997;1:363-377.

[54] Lobregt S, Viergever MA. A discrete dynamic contour model. IEEE Trans Image Process 1995;14:12-24.

[55] Pardo XM, Radeva P, Cabello D. Discriminant snakes for 3D reconstruction of anatomical organs. Med Image Anal 2003;7:293-310.

[56] Yang J, Tong L, Faraji M, et al. IVUS-Net: An intravascular ultrasound segmentation network. Lecture Notes in Computer Science (11010): Smart Multimedia–ICSM 2018. Springer, Cham 2018;367-377.

[57] Gu S, Chen Y, Sheng F, et al. A novel method for breast mass segmentation: from superpixel to subpixel segmentation. Mach Vis Appl 2019;30:1111-1122.

[58] Wang R, Ma Y, Sun W, et al. Multi-level nested pyramid network for mass segmentation in mammograms. Neurocomputing 2019;363:313-320.

[59] Rhim H, Dodd III GD. Radiofrequency thermal ablation of liver tumors. J Clin Ultrasound 1999;27:221-229.

[60] Martin HE, Ellis EB. Biopsy by needle puncture and aspiration. Ann Surg 1930;92:169.

[61] Mwikirize C, Nosher JL, Hacihaliloglu I. Learning needle tip localization from digital subtraction in 2D ultrasound. Int J Comput Assist Radiol Surg 2019;14:1017-1026.

[62] Redmon J, Farhadi A. YOLO9000: better, faster, stronger. 2017 IEEE Conference on Computer Vision and Pattern Recognition (CVPR). 2017;6517-6525.

[63] Mwikirize C, Nosher JL, Hacihaliloglu I. Single shot needle tip localization in 2D ultrasound. Lecture Notes in Computer Science (11768): Medical Image Computing and Computer Assisted Intervention–MICCAI 2019. Springer, Cham 2019;637-645.